International Journal of Railway Research, Vol. 8, No. 2, (2022), 21-32

Iran University of Science and Technology

International Journal of

Railway Research

Analysis of wheel and rail Hertzian and Non-Hertzian contact theories using UM software considering the effect of rail inclination on wheel wear

M.Aziznia[1], A. Owhadi.[2], M. Shadfar[3]

[1]B.sc of Rolling Stocks, Faculty of Railway Engineering, Iran University of Science and Technology, milad_aziznia@moein-ig.ir

[2]A.Professor, Faculty of Railway Engineering, Iran University of Science and Technology, aohadi@iust.ac.ir

[3]Ph.D. student of Rolling Stocks, Faculty of Railway Engineering, Iran University of Science and Technology, morad_shadfar@rail.iust.ac.ir

ARTICLE INFO

Article history:
Received: 14.03.2022
Accepted: 04.04.2022
Published: 06.04.2022

Keywords:
Wear
Contact theories
Wheel
Rail
Simulation
Bogie
UM

A B S T R A C T

Wheel-rail interaction has always been one of the issues in the railway industry. In this paper, the effect of Hertzian and non-Hertzian contact theories on the wheel wear due to the rail inclination was investigated. by using the UM software.

According to the results, longer contact areas are obtained in non- Hertzian contact theory compared to Hertzian contact theory. In non-Hertzian contact areas, the wear band and wear depth in the areas near the flange were decreased with increase rail inclination, while it was opposite in Hertzian contact areas.The distribution of wheel and rail contact points in the Hertzian contact is scattered in the final wheel profile, while in non-Hertzian contact the accumulation of the contact points is observed.

Introduction

The forces and vibrations on the rail and the rail vehicle are generally caused by the contact forces created and the interaction between the wheel and the rail. Proper performance of this set has a direct impact on the performance of other components. The presence of any local defects or deterioration such as wear and fatigue will reduce the efficiency of the collection. For this reason, many scientists have tried to control and prevent the occurrence or spread of defects by predicting and examining the contact forces. One of these defects is wheel wear, which is one of the most important defects due to the cost of wheel production. Scientists have studied this important issue using various modeling. In 1993, Kalousek and Grassie considered the unevenness of the rail and concluded that the main cause of wear in rails with short step unevenness is longitudinal slip. Also, the amount of removal material was declared as a factor of severe wear

*Corresponding author: Assistant professor A. Ohadi
Email address: aohadi@iust.ac.ir

[DOI: 10.22068/ijrare.296]

mode, and it was considered as the result of the work of friction force.[1]

Wheel and rail interaction, effective elements in contact mechanics, contact model of two contact bodies, and tribological properties are the items that have been considered in analytical modeling to investigate the amount of material wear. In these researches, some scientists have considered rail profiles as fixed for ease of work, and have focused their studies on wheel profiles. Also, for further simplification, the relationship between wear and friction work is often considered linear. [2]

In 2002, Zakharov et al. Derived the wheel and rail wear equations to achieve the wheel wear rate for the optimal wheel profile, taking into account the effective parameters of wear in the two bodies involved.[2]

In the last ten years, the amount of removal material has been calculated using algorithms such as CONTACT and FASTSIM in which the contact forces have been investigated. In 2005, for example, Ayasse and Chollet invented a method in which they measured the maximum contact area pressure in different bands separately by tape measurement, which became a relatively accurate contact area and registered a new algorithm called STRIPES.[3]

In 2008, Enblom and Berg examined the wear rate by estimating the contact area and pressure distribution and achieved results such as shifting the material removal rate to the flange. In this research, he used the results obtained from the MBS Gensys code in the Hertzian contact model and the non-hertz approach with the Kalker contact model. [4]

In 2009, Piotrowski and Kik modeled the pressure distribution in the direction of rotation, assuming a semi-elliptical pressure distribution, and were able to calculate the natural pressure at the point of contact by satisfying the contact conditions. They also concluded that the CONTACT codes provided by Kalker could be used with confidence, thus reaching the Multi-Body System codes, and their method became known as the Kik-Piotrowski method.[5]

In 2014, Sichani et al. Used analytical modeling in elliptic contact cases with results similar to Hertz results, and in non-elliptical cases with results close to the exact and expensive calculator method (CONTACT code). They also achieved better contact area and more accurate pressure distribution and ANALYN algorithm compared to simple non-elliptical methods based on virtual penetration.[6]

In 2016, Liu, Bruni, and Vollebregt improved the CONTACT algorithm by examining the effect of the wheel yaw angle on the wheel-rail contact area.[14]

In 2019, Boyang An and colleagues compared and evaluated four methods of the Kik-Piotrowski contact model, the Linder method, the Ayasse-Chollet's STRIPES algorithm, and the Sichani's ANALYN algorithm, to evaluate non-Hertzian methods for wear prediction. They used the Archard abrasion model and USFD abrasion model in modeling and adjusted their creep force algorithm based on FASTSIM and FaStrip algorithms. They concluded that ANALYN + FaStrip had a higher response speed than other methods and that STRIPES + FASTSIM was more accurate in predicting the maximum wear depth for the USFD wear model.[7]

Hertzian and Non-Hertzian contact

In the case of rigid contact, it is only possible to contact one point of the wheel with the rail. By applying the deformations caused by the initial point of contact, it will be possible to contact other points as well. The deformation at the initial contact point allows the wheel and rail profiles to be deformed and compressed, and thus, at the same time as the initial contact points, other points in the wheel-rail interaction. Hertz in her theory assumed that two objects at the point of contact have a fixed radius of curvature, and therefore the contact surface obtained in the action of the wheel and rail is known as the Hertz ellipse. The radius of curvature of the wheel and rails at the point of contact changes for certain lateral displacements of the axle. In this case, the resulting contact surface will be different from the ellipse. The obvious difference in the shape and dimensions of the contact surface in this case compared to the Hertzian contact in the case where the contact area has a variable radius of curvature causes a non-Hertzian contact. Figure 1 shows the difference between contact areas and along the way for these two contact theories.

[DOI: 10.22068/ijrare.296]

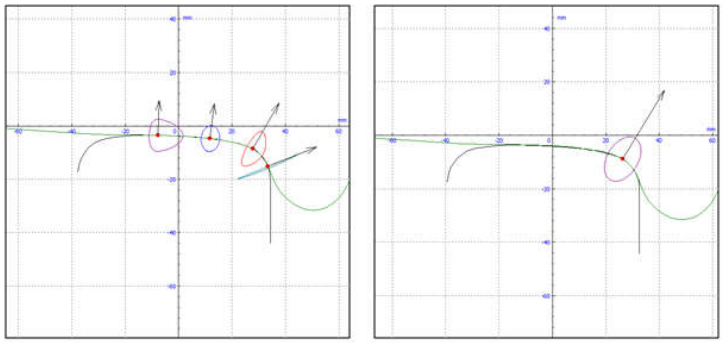

b a

Figure 1. Wheel and rail contact areas in a curve
a. Hertzian contact theory b. Non-Hertzian contact theory

In wheel and rail contact, the goal is to obtain the actual contact area and the amount of pressure in that area. For this purpose, the following contact equation is used to obtain the boundaries of the contact area:

$$\frac{x^2}{2R} + f(y) = \delta - u(x,y) \quad (1)$$

Where $f(y)$ is the natural distance in the transverse direction around the point of contact, R is the radius of the wheel at the point of contact, $u(x,y)$ is the elastic deformation function, and δ is the amount of elastic deformation caused by the contact. There is no direct solution to Equation (1) because the elastic deformation $u(x,y)$ depends on the pressure in the contact area. Therefore, to solve it, by obtaining the rest of the elements of the equation from the methods performed by Kalker [9] and Knothe [10], and by dividing the contact area in Hertz and according to the amount of pressure can be done as follows: [7]

$$p(x,y) \begin{cases} = 0 & \text{Outside the contact area} \\ > 0 & \text{In the contact area} \end{cases} \quad (2)$$

Depending on the amount of load, the value δ will need to be optimized.

In the non-Hertzian contact, according to the optimized Kik-Piotrowski algorithm to prevent the calculation of elastic deformation, the contact area boundaries are presented as Equation: [3]

$$g(y) = \varepsilon\delta - f(y) \geq 0 \quad (3)$$

Where ε is a coefficient whose value is assumed to be 0.55, assuming that the contact area in the direction of wheel motion is semi-elliptical. The boundary value of the contact area according to Equation (4) is:

$$a(y) \approx \sqrt{2R \cdot g(y)} \quad (4)$$

According to Equation 3, $g(y)$ is a function of the boundaries of the contact area.

After initializing the contact area, the shape of the contact area should be obtained more precisely.

The maximum pressure inside the contact area is obtained from the contact conditions. At the point of contact, the amount of elastic deformation due to wheel and rail contact is δ. therefore:

$$p_0 = N\sqrt{2R \cdot \varepsilon\delta}\left(\iint_C \sqrt{a^2(y) - x^2}\,dxdy\right)^{-1} \quad (5)$$

Where the amount of force N is obtained from Equation (6):

[DOI: 10.22068/ijrare.296]

$$N = \frac{\pi E \delta}{2(1-\mu^2)} \left(\iint_C \frac{\sqrt{a^2(y)-x^2}}{\sqrt{y^2+x^2}} dxdy \right)^{-1} \times \iint_C \sqrt{a^2(y)-x^2}\, dxdy \quad (6)$$

Where μ and E are the Poisson's ratio and the modulus of elasticity, respectively. Finally, the equation of pressure distribution in the contact area as equation (7) is: [7]

$$p(x,y) = \frac{p_0}{a(0)} \sqrt{a^2(y)-x^2} \quad (7)$$

Dynamic modeling

Dynamic UM software version 8 was used for modeling. This software has various capabilities and modules for various types of rail system analysis and calculates the wear problem by considering different theories.

In this research, an open-top freight wagon equipped with 18-100 Russian bogies was modeled, because this bogie is widely used in Iran's railway. S1002 wheel profile, UIC 60 rail profile, and 1:20 and 1:40 rail inclination was considered. The effects of rail irregularities and lubrication in the curves were ignored at this stage. The railway line was used with the statistical average of the distribution of various curves in the Iran's railway. Track details are provided in Table 1.

Table 1. Weighted values of Track [12]

	radius	weight coefficient	spiral (mm)	cant (mm)	speed (Km/h)
tangent	-	0.8400	0.00	0	40
curve	250	0.0088	60.00	150	42.63
curve	300	0.0107	60.00	130	47.89
curve	400	0.0181	60.00	100	53.15
curve	500	0.0108	53.00	100	58.42
curve	600	0.0081	44.17	85	63.68
curve	700	0.0042	37.86	75	66.31
curve	750	0.0009	35.33	75	68.94
curve	800	0.0098	33.13	64	74.21
curve	900	0.0002	29.44	33	79.47
curve	1000	0.0213	26.5	30	90.00
curve	1200	0.0673	22.08	25	90.00

In the contact between wheels and rails, the value of Poisson's coefficient was 0.3 and the modulus of elasticity was 210 GPa.

Table 2 describes the input parameters in UM software for Hertzian and non-Hertzian contact area modeling.[12]

Table 2. Input parameters for wheel-rail contact modelling.

Parameter	value	Parameter	value
Tape circle distance	1.435 m	Rail profile	UIC60
Wheel radius	0.478 m	Wheel profile	candidates
Rail inclination	1:20 1:40	Critical speed for creep	0.1 m.s^{-1}
Young Modulus	210 Gpa	Poisson ratio	0.3
Number of strips	10	Number of elements on contact patch	32
Interpenetration factor on non-Hertrzian contact (ε)	0.55		

Archard's modified theory called Specht was used to calculate wear. This theory is similar to the method used by Zobory, which uses two wear modes to analyze wheel and rail wear. [15] The basis of Equation (8) is based on the linear relationship between the work of friction force and the volume of the worn material.[11]

In UM software, the method of measuring the amount of wheel and rail wear is used, which has a high accuracy compared to other options, the relationship of which is in the form of relationship (8). [11]

$$\begin{cases} I = k_V A, & w < w_{cr} \\ I = k_V \alpha A, & w \geq w_{cr} \end{cases} \quad (8)$$

Where is the volume of the worn material m^3 , A is the force of friction J , k_V is the index of wear m^3/J , w is the power of friction W/m^2 , and finally w_{cr} is the critical power density W/m^2 .

Table 3 shows the necessary factors to calculate the amount of worn material based on the Specht Wear model.[12]

Table 3. Values for wear calculation.

Parameter	value
Wear factor	1E-13 m^3.J^{-1}
Jumping Factor	10
Critical power density	4 W.mm^{-2}

[DOI: 10.22068/ijrare.296]

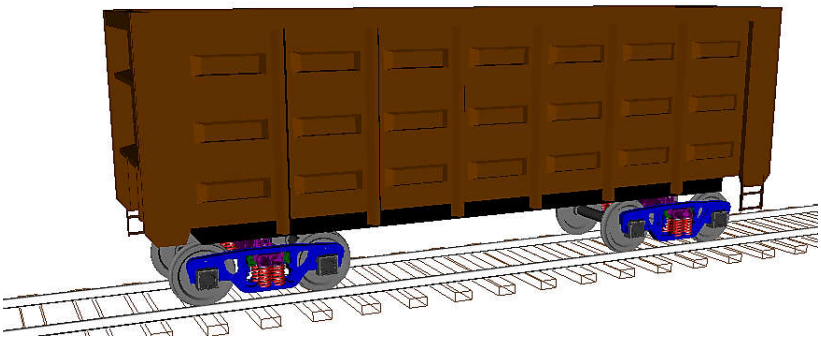

figure 2. The wagon used in the simulation

Results and analysis

According to the conditions mentioned (Figure 2), the wagon was traveled 230 times on the test route according to Table 1, and in total, the distance was 6000 km. It should be noted that wear modeling in dynamic software is of the accelerated type, and this distance will be a much larger number. The results of two Hertzian and non-Hertzian solutions for the 1:20 and 1:40 rail inclination is shown in Figures 3 and 4.

The distribution of contact points and the rolling radius difference of the wheel, which indicates the dynamic performance of the wheel, is a function of the geometry of the wheel and the rail and is independent of the calculation of forces in contact theory. Therefore, only a change in contact theory by maintaining the geometry and distribution of wheel and rail contact points has led to significant changes in the results. This highlights the importance of using more advanced contact theories in analysis; Because the higher the accuracy of the contact theory for measuring the contact area, the higher the wear accuracy will be, and as a result, the distribution of contact points and the difference in the rolling radius will be examined more accurately.

Another important point is how Hertzian and non-Hertzian contact theories affect the deformation of the rolling radius difference curve and the distribution of contact points on the wear profile. In general, this is normal because, with wheel wear, the wheel profile loses its original shape and causes the contact points to scatter.

Figures 3 to 7 show the distribution of contact points and the changes in the rolling radius difference with the lateral displacement of the wheel on the rail in the case of new and worn wheel profiles under Hertzian and non-Hertzian contact theories.

From the comparison of Figures 3 to 7, it can be seen that the effect of Hertzian contact theory on the wheel profile causes the scattering of contact points between the wheel and the rail; While Non-Hertzian contact theory focuses on contact points. This difference can be considered as the number of contact points more and closer to each other in the theory of non-Hertzian contact, because according to Figure (1.a) there is only one point of contact in the hertz contact, and this causes the contact points in the contact of the wheel surface to expand. (Figures 4.a and 6.a)

Also, due to wheel wear, the rolling radius difference in both Hertzian and non-Hertzian contact modes changes abruptly, and these changes apply to both rail inclinations. It should be noted that this is directly related to the increase in wear depth in the area near the flange, and if the changes in the rolling radius of the wheel in the area near the flange are large, it will cause a lot of damage to the rail; Because it causes the rail contact with the wheel suddenly and increases the probability of deviating from the track.

[DOI: 10.22068/ijrare.296]

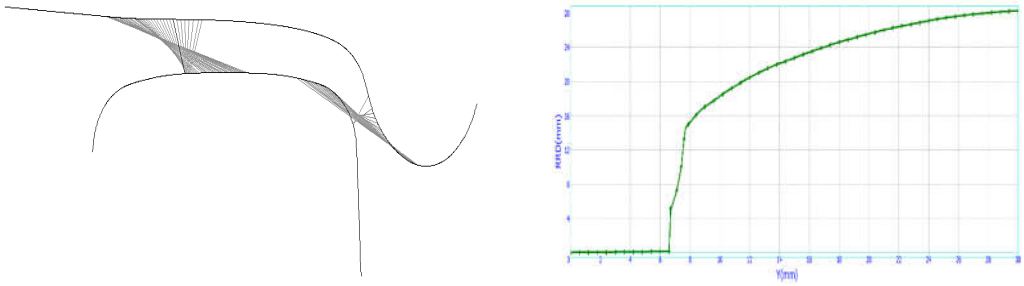

a b

Figure 3. Distribution of contact points (a) and wheel rolling radius difference curve (b) for new S1002 wheel profile and new UIC rail

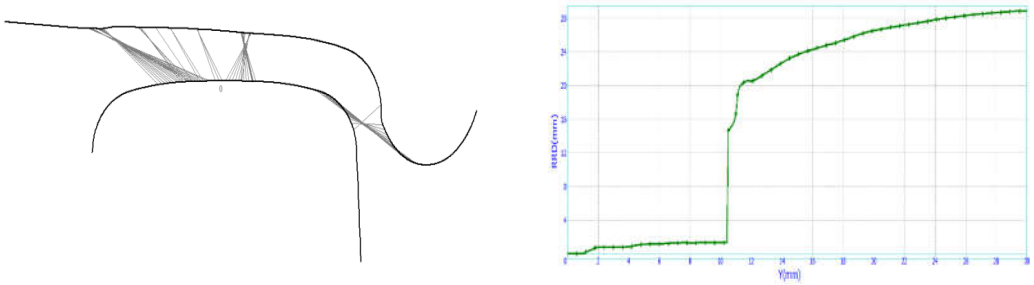

a b

Figure 4. Distribution of contact points (a) and the difference curve of the rolling radius of the worn wheel (b) in Hertzian contact for the 1:20 rail inclination

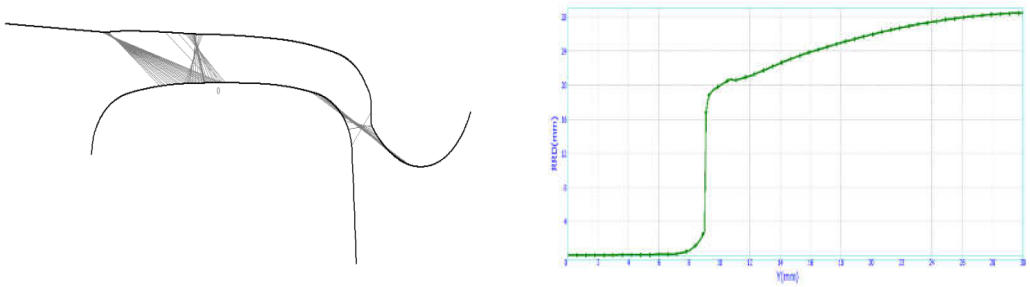

a b

Figure 5**.** Distribution of contact points (a) and the difference curve of the rolling radius of the worn wheel (b) in non-Hertzian contact for the 1:20 rail inclination

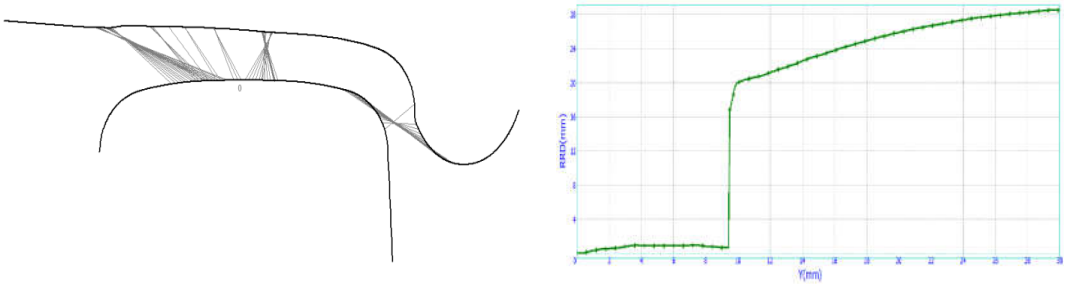

a b

Figure 6. Distribution of contact points (a) and the difference curve of the rolling radius of the worn wheel (b) in Hertzian contact for the 1:40 rail inclination

[DOI: 10.22068/ijrare.296]

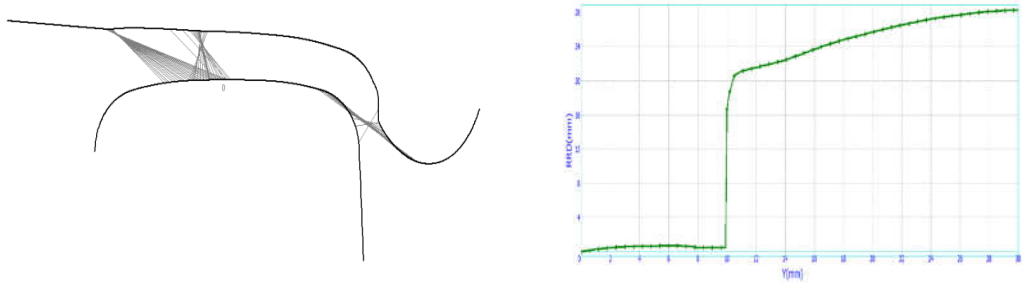

a b

Figure 7. Distribution of contact points (a) and the difference curve of the rolling radius of the worn wheel (b) in non-Hertzian contact for the 1:40 rail inclination

One of the points to be noted is the geometric dimensions of the contact area in both Hertzian and non-Hertzian contact. It should be noted that in the improved Kik-Piotrowski algorithm for solving the non-Hertzian contact problem, the shape of the contact area is integrated and with a point of contact, which significantly increases the accuracy of problem-solving.

The dimensions of the contact areas based on Hertz calculations and solving the corresponding equations [7] are shown in Figure 8. Figure 8.a shows the dimensions of the contact area in the Hertzian contact for moving in a tangent track, and Figure 8.b shows the dimensions of the contact area in the Hertzian contact for crossing the curve. Figures 8.c, 8.d, and 8.e also show the dimensions of the contact area in non-Hertzian contact for moving in a tangent track and crossing the curve.

As shown in Figure 8, for the rail inclination 1:20, the wheel wear rate is significantly reduced by changing the mode of the contact model from Hertzian to non-Hertzian contact, so that the maximum amount of wheel wear that occurs in the wheel flange area is In the Hertzian contact, it reaches 3.3 mm in the left wheel and 3.5 mm

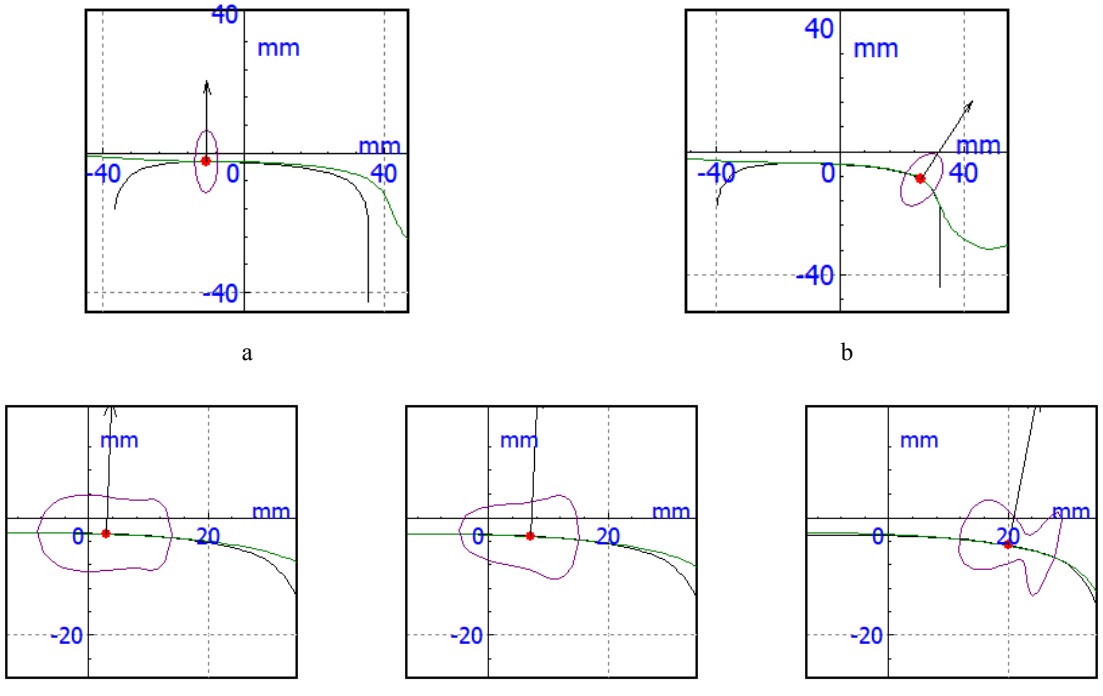

a b

c d e

Figure 8. Dimensions of the contact area in Hertzian contact (a and b) and non-Hertzian contact (c, d, e)

[DOI: 10.22068/ijrare.296]

in the right wheel, but in the non-Hertzian contact, this amount reaches about 1.6 mm in the left wheel and 2 mm in the right wheel. Another important result is that the worn area on both wheels in the non-Hertzian contact is significantly reduced compared to the Hertzian contact, and this decrease can be due to the distribution of normal contact force at different points on the wheel areas caused by the model. The call is non-Hertzian. This is important from the results that Braghin and colleagues obtained with mathematical modeling as well as laboratory tests and simulations performed to predict wheel wear. [15]

As can be seen in Figures 9 and 10, the results for the 1:40 rail inclination are slightly different from the 1:20 rail inclination. This amount of difference is such that for the slope under the rail 1:40 in the non-Hertzian contact, the amount of wear in the flange area is more than the Hertz contact. Figures 11 and 12, which show the amount of wheel wear in the Hertzian and non-Hertzian contact theories for the rail inclinations, are evidence of this.

Table 4 shows the maximum depth of right wheel wear that occurred near the wheel flange area in different contact theories for the different rail inclinations. If the geometry of the track and the path is symmetrical, the choice of the wheel

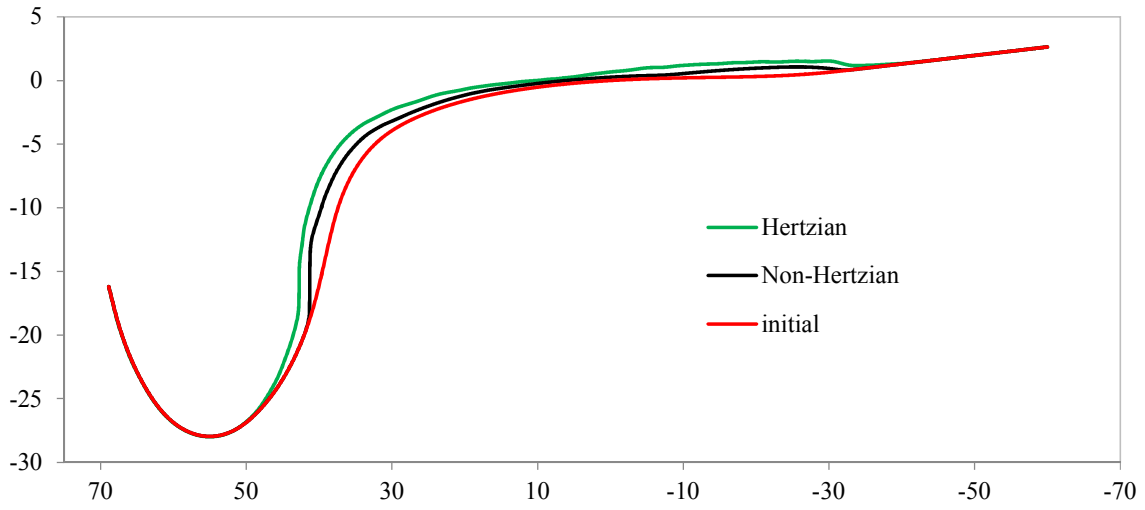

Figure 9. Diagram of a worn wheel in the theory of hertz contact and non-hertz contact for the right wheel on 1:20 rail inclination

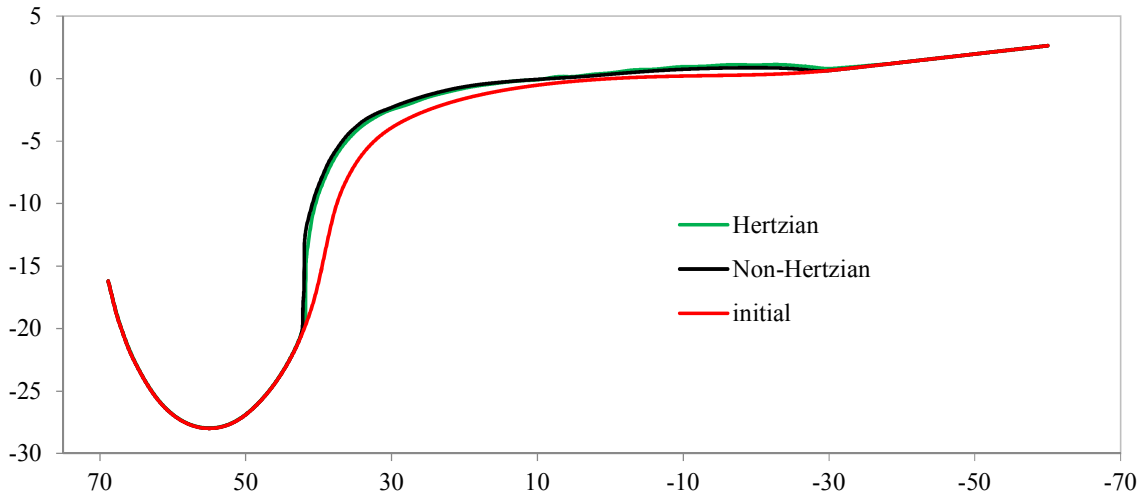

Figure 10. Diagram of a worn wheel in the theory of hertz contact and non-hertz contact for the right wheel on 1:40 rail inclination

[DOI: 10.22068/ijrare.296]

does not matter much, but the counter-clockwise of the steep curves (curves with a smaller radius) led the right wheel to be chosen as the wheel in this problem. It should be noted that these curves are defined according to Table 4.

Table 4. Maximum depth of right wheel wear (mm)

Rail inclination	Hertzian contact	Non-Hertzian contact
1:20	3.521	1.968
1:40	2.356	2.925

According to Figures 7 and 9, for the 1:40 rail inclination, the amount of reduction of wear area in the Hertzian contact is very small compared to the 1:20 rail inclination, but the wear depth in the non-Hertzian contact in the area near the flange is significantly increased. The maximum wear depth in the Hertzian contact on the right wheel is about 2.3 mm, and in the non-Hertzian contact, it is about 2.9 mm. But in the left wheel, this amount of wear is less, and the reason is the geometry of the path and the counter-clockwise of the steep curves, which causes less wear on the left wheel.

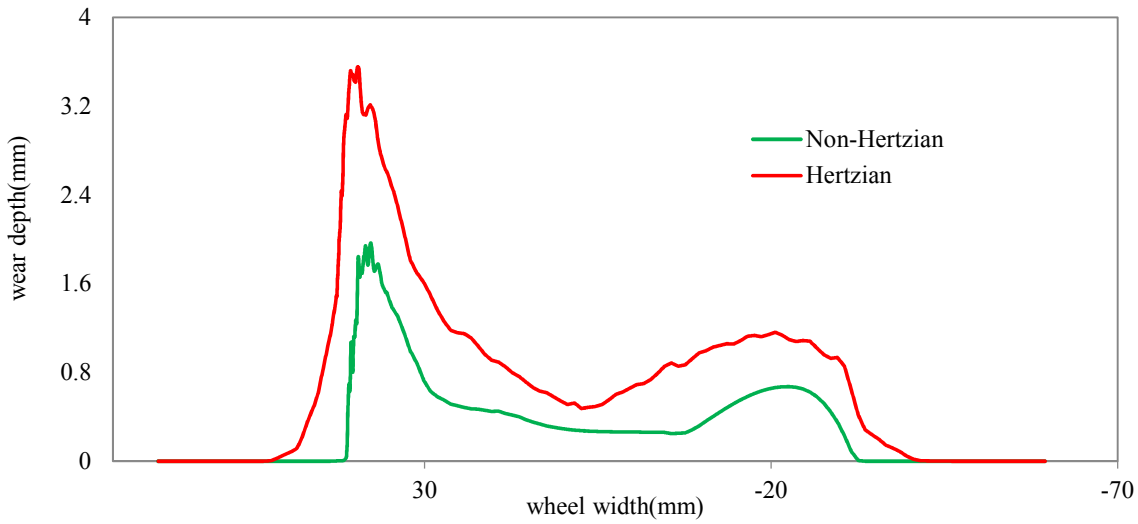

Figure 11. Wheel wear rate diagram in the theory of hertz contact (red) and non-hertz contact (green) for 1:20 rail inclination

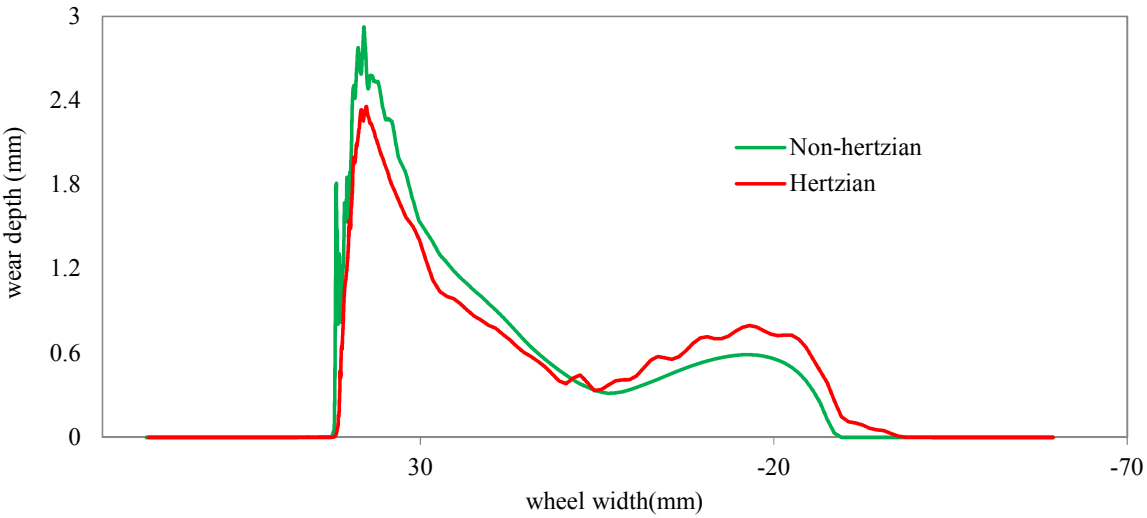

Figure 12. Wheel wear rate diagram in the theory of Hertzian contact (red) and non-Hertzian contact (green) for 1:40 rail inclination

[DOI: 10.22068/ijrare.296]

The results obtained from the 1:40 rail inclination shown in Figure 12 are very similar to the results presented by Berg and Enblom [4], But the results of the 1:20 rail inclination contradict their results. Because the amount of wheel wear in the Hertzian and non-Hertzian contact theories on the 1:20 rail inclination is more than the amount of wheel wear on the 1:40 rail inclination. The two researchers, who used the 1:30 rail inclination in their paper, concluded that the non-Hertzian contact areas in the conformal contact create a larger wear band, so in analyzing wheel and rail wear problems, especially In the presence of high slip fields (increased friction force work) or high values of vertical force (increased vertical contact stresses), the use of modern non-Hertzian theories in the analysis produces quite different results, although the general pattern wear is constant. [4]

To calculate wheel wear, Roger and his companion traveled the simulated rail vehicle in a curve with a radius of 600 and 1,500 m, as well as a tangent track. Figure 13 shows the research of Roger et al., Which shows the difference in wheel wear depth in a 600 m radius curve in both Hertzian and non-Hertzian contact. The results obtained in the current study for the 1:40 rail inclination is completely consistent with Roger's results.

Figure 13 shows the results of a curve with a radius of 600 m as a steeper curve.

To verify the results and diagrams of this study, Barghin laboratory tests were used, which used two rollers to examine wheel and rail wear. [13]

As can be seen in Figure 14, the diagrams obtained from this study are similar to the diagrams obtained from the research of Barghin et al.

This evidence indicates that the difference and accuracy of measuring wheel wear depth per kilometer in this study compared to Barghin research is less than 5%, which shows the accuracy of the data obtained.

Among the results obtained in this research is the effect of changing the rail inclination on the amount of worn material in different contact theories; Thus, although the non-Hertzian contact areas in the contour contact create a larger wear band for the 1:40 rail inclination, the 1:20 rail inclination, the Hertzian contact areas produce a larger wear band. Therefore, the analysis of wheel and rail wear problems, especially in the presence of high slip fields (increase in friction force work) or high values of vertical force (increase in vertical contact stresses), in addition to using modern non-Hertzian theories in the analysis, Attention was also paid to the rail inclination, because even with a constant wear pattern, the results would be too much. Therefore, for the theory of non-Hertzian contact, with increasing the rail inclination, the wear band and the wear depth

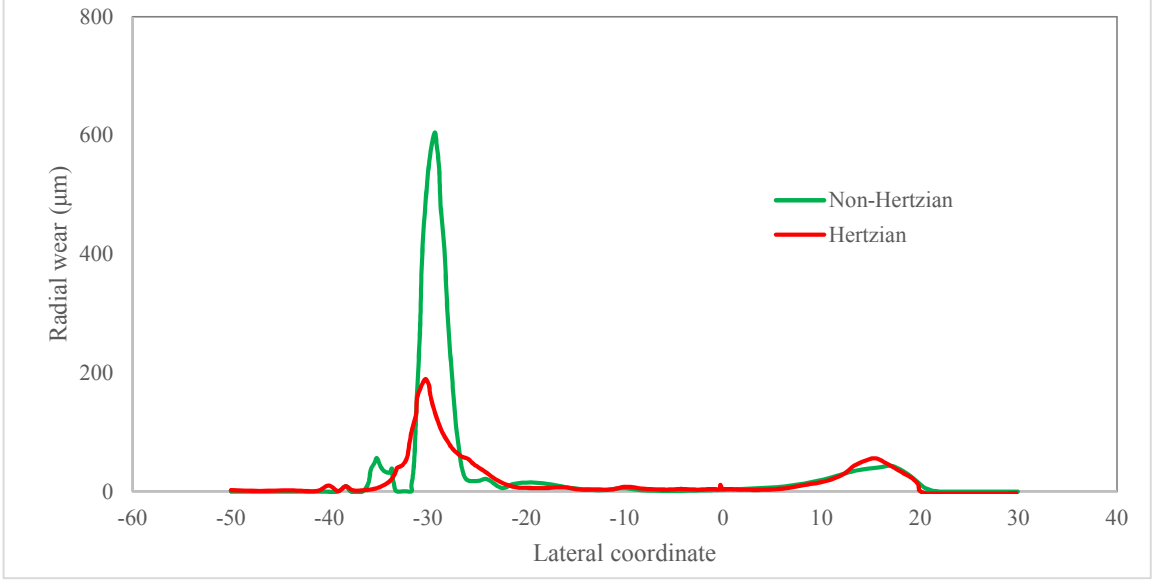

Figure 13. Results were obtained by Roger and colleagues for wheel wear in a 600 m curve.

[DOI: 10.22068/ijrare.296]

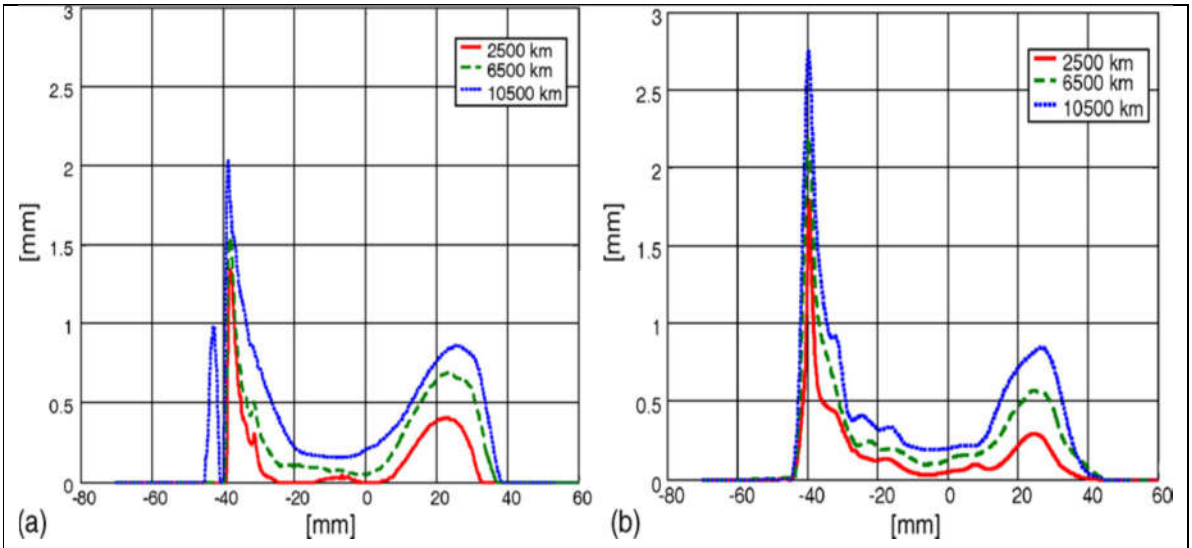

Figure 14. The results of laboratory tests (a) and mathematical calculations (b) performed by Barghin.

decreases in the area near the flange; However, in Hertzian contact, the wear band increases with increasing rail inclination and the wear depth increases in the area near the flange.

Conclusion

In this research, using UM software, the wear depth of the wheel with S1002 profile was calculated for railway lines with UIC60 profile and 1:20 and 1:40 rail inclination using Hertzian and non-Hertzian contact theories. The results obtained are:

- In non-Hertzian contact theory, larger contact areas are obtained compared to Hertzian contact theory.
- In non-Hertzian contact areas, with increasing rail inclination, the wear band decreases and the wear depth in the area near the flange also decreases.
- In Hertzian contact areas, with increasing rail inclination, the wear band and wear depth in the area near the flange also increases.
- The distribution of wheel and rail contact points in the Hertzian contact is scattered in the final wheel profile, while in non-Hertzian contact the focus of the contact points is observed.
- In non-Hertzian contact, the focus is on the contact points, which increases the wear band.
- Wheel radius difference changes in both Hertzian and non-Hertzian theory in worn profiles change abruptly.

References

[1] Xie, G., & Iwnicki, S. D. (2008). Calculation of wear on a corrugated rail using a three-dimensional contact model. *Wear*, *265*(9-10), 1238-1248.

[2] Zakharov, S., & Zharov, I. (2002). Simulation of mutual wheel/rail wear. *Wear*, *253*(1-2), 100-106.

[3] Ayasse, J. B., & Chollet, H. U. G. U. E. S. (2005). Determination of the wheel rail contact patch in semi-Hertzian conditions. *Vehicle System Dynamics*, *43*(3), 161-172.

[4] Enblom, R., & Berg, M. (2008). Impact of non-elliptic contact modelling in wheel wear simulation. *Wear*, *265*(9-10), 1532-1541.

[5] Piotrowski, J., & Kik, W. (2008). A simplified model of wheel/rail contact mechanics for non-Hertzian problems and its application in rail vehicle dynamic simulations. *Vehicle System Dynamics*, *46*(1-2), 27-48.

[6] Sh. Sichani, M., Enblom, R., & Berg, M. (2014). A novel method to model wheel–rail normal contact in vehicle dynamics simulation. *Vehicle System Dynamics*, *52*(12), 1752-1764.

[7] An, B., Ma, D., Wang, P., Zhou, J., Chen, R., Xu, J., & Cui, D. (2020). Assessing the fast non-Hertzian methods based on the simulation of wheel–rail rolling contact and wear distribution. *Proceedings of the Institution of Mechanical Engineers, Part F: Journal of Rail and Rapid Transit*, *234*(5), 524-537.

[DOI: 10.22068/ijrare.296]

[8] A.Asadi, A.R.Falah (2008)," Determination of wheelset contact constraints with rails by geometric method", *Journal of Transportation*, *5*(2),167-175

[9] Kalker, J. J. (2000). Rolling contact phenomena. In *Rolling contact phenomena* (pp. 1-84). Springer, Vienna.

[10] Knothe, K., & Le The, H. (1984). A contribution to the calculation of the contact stress distribution between two elastic bodies of revolution with non-elliptical contact area. *Computers & Structures*, *18*(6), 1025-1033.

[11] W.Specht, New particulars of Wear of Heavy Railway Carriage Wheels // Glasers Annalen, 1987, Vol. 9. P. 271–280.

[12] Molatefi, H., Mazraeh, A., Shadfar, M., & Yazdani, H. (2019). Advances in Iran railway wheel wear management: a practical approach for selection of wheel profile using numerical methods and comprehensive field tests. *Wear*, *424*, 97-110.

[13] Braghin, F., Lewis, R., Dwyer-Joyce, R. S., & Bruni, S. (2006). A mathematical model to predict railway wheel profile evolution due to wear. *Wear*, *261*(11-12), 1253-1264.

[14] Liu, B., Bruni, S., & Vollebregt, E. (2016). A non-Hertzian method for solving wheel–rail normal contact problem taking into account the effect of yaw. *Vehicle System Dynamics*, *54*(9), 1226-1246.

[15] Liu, B., & Bruni, S. (2020). Comparison of wheel–rail contact models in the context of multibody system simulation: Hertzian versus non-Hertzian. *Vehicle System Dynamics*, 1-21.

[DOI: 10.22068/ijrare.296]